Resonant X-Ray Scattering on the M-Edge Spectra from Triple-k Structure Phase in $U_{0.75}Np_{0.25}O_2$ and UO_2

Tatsuya Nagao* and Jun-ichi Igarashi¹

Faculty of Engineering, Gunma University, Kiryu, Gunma 376-8515

¹ Faculty of Science, Ibaraki University, Mito, Ibaraki 310-8512

(Received September 14, 2018)

We derive an expression for the scattering amplitude of resonant x-ray scattering under the assumption that the Hamiltonian describing the intermediate state preserves spherical symmetry. On the basis of this expression, we demonstrate that the energy profile of the RXS spectra expected near U and Np M_4 edges from the triple-**k** antiferromagnetic ordering phase in UO₂ and U_{0.75}Np_{0.25}O₂ agree well with those from the experiments. We demonstrate that the spectra in the σ - σ' and σ - π' channels exhibit quadrupole and dipole natures, respectively.

KEYWORDS: resonant x-ray scattering, triple-k antiferromagnetic ordering, UO2, NpO2, U0.75Np0.25O2

1. Introduction

Resonant x-ray scattering (RXS) data obtained from actinide compound around the $M_{4,5}$ edges supply invaluable information of the properties of the 5f state, $^{1-4}$ since the scattering process consists of $3d \rightarrow 5f$ transition in the dipolar (E1) process. Recently, we have derived an useful expression for the scattering amplitude of RXS under the assumption that the Hamiltonian describing the intermediate state preserves the rotational invariance.⁵ Our theory explicitly treats the energy dependence of the scattering amplitude in contrast with the previous theory employing the fast collision approximation.^{6–8} This expression is particularly convenient for analyzing the energy profile of the RXS spectra from actinide $M_{4.5}$ edges such as NpO₂, URu₂Si₂ and so on.^{5,9} In this paper, we apply the result to investigate the RXS spectra near U and Np M_4 edges from the ordered phase in UO₂ and U_{0.75}Np_{0.25}O₂.^{10,11} Analysis of the RXS spectra in these compounds suggested to show the complicated ordering patterns such as the triple-k type ones gives useful information complementary to that from the neutron scattering experiment.

Known actinide dioxides exhibit the cubic CaF₂ crystal structure (F_{m3m}) at room temperature. Experiments have confirmed that both UO_2 and $U_{0.75}Np_{0.25}O_2$ behave as antiferromagnets (AFM) below $T_N = 30.8 \text{ K}$ and ≈ 17 K, respectively, having transverse triple-k structure with modulation vector $\mathbf{Q} = (001)^{10,12,13}$ On the other hand, recent RXS experiments have suggested longitudinal triple-k antiferroctupolar (AFO) ordering phase is plausible in NpO_2 below $T_0 = 25.5$ K with the same modulation vector.^{3,14–17} In our previous work⁵ we have investigated the RXS spectra expected from the longitudinal type of the triple-k AFO phase in NpO₂ and obtained fairly good agreement with the experiments. As we shall show, two types of the energy profile of the spectra $(\alpha_1(\omega))$ and $\alpha_2(\omega)$ in Eq. (2.1) are expected from the triple-k AFM ordering phase, while only one type of that $(\alpha_2(\omega))$ emerges from the triple-**k** AFO ordering phase. In this work, we concentrate on the former case paying

attention to the difference between the spectra at U and Np sites, namely, between the f^2 and f^3 configurations.

2. RXS Amplitude

Since we are interested in the 5f electron systems in which a localized picture gives reasonable description, we suppose the initial state at the site j is spanned by the states within ground multiplet J as $|0\rangle_j = \sum_{m=-J}^{J} c_j(m)|J,m\rangle$. An incident photon with energy $\hbar\omega$, wave vector \mathbf{k} , and polarization $\boldsymbol{\epsilon}$ excites an electron in core 3d level into the unoccupied 5f state, then the excited electron falls into the core level emitting a scattered photon with energy $\hbar\omega$, wave vector \mathbf{k}' , and polarization $\boldsymbol{\epsilon}'$ in the E1 process around the actinide $M_{4.5}$ edges.

When the Hamiltonian describing the intermediate state of the scattering process preserves the spherical symmetry, the expression of the RXS amplitude reduces to an extremely simple form.⁵ This condition is justified when the crystal electric field (CEF) Hamiltonian and the inter-site interaction are negligible compared with the energy scale of the intermediate state. Then, the RXS amplitude at the site j is summarized as⁵

$$M_{j}(\boldsymbol{\epsilon}', \boldsymbol{\epsilon}, \omega) = \alpha_{0}(\omega)\boldsymbol{\epsilon}' \cdot \boldsymbol{\epsilon} - i\alpha_{1}(\omega)(\boldsymbol{\epsilon}' \times \boldsymbol{\epsilon}) \cdot \langle 0|\mathbf{J}|0\rangle + \alpha_{2}(\omega)\sum_{\nu} P_{\nu}(\boldsymbol{\epsilon}', \boldsymbol{\epsilon})\langle 0|z_{\nu}|0\rangle, \qquad (2.1)$$

where quadrupole operators are represented as $z_1 \equiv Q_{x^2-y^2} = (\sqrt{3}/2) \ (J_x^2 - J_y^2), \ z_2 \equiv Q_{3z^2-r^2} = (3J_z^2 - J(J+1))/2, \ z_3 \equiv Q_{yz} = (\sqrt{3}/2) \ (J_yJ_z + J_zJ_y), \ z_4 \equiv Q_{zx} = (\sqrt{3}/2) \ (J_zJ_x + J_xJ_z), \ \text{and} \ z_5 \equiv Q_{xy} = (\sqrt{3}/2) \ (J_xJ_y + J_yJ_x).$ The geometrical factors are defined as $P_1(\epsilon', \epsilon) = (\sqrt{3}/2)(\epsilon'_x\epsilon_x - \epsilon'_y\epsilon_y), \ P_2(\epsilon', \epsilon) = (2\epsilon'_z\epsilon_z - \epsilon'_x\epsilon_x - \epsilon'_y\epsilon_y)/2, \ P_3(\epsilon', \epsilon) = (\sqrt{3}/2)(\epsilon'_y\epsilon_z + \epsilon'_z\epsilon_y), \ P_4(\epsilon', \epsilon) = (\sqrt{3}/2)(\epsilon'_z\epsilon_x + \epsilon'_x\epsilon_z), \ \text{and} \ P_5(\epsilon', \epsilon) = (\sqrt{3}/2)(\epsilon'_x\epsilon_y + \epsilon'_y\epsilon_x).$ Here, we have suppressed the dependence on the site j in the right hand side of Eq. (2.1). Three independent energy profiles $\alpha_0(\omega), \alpha_1(\omega)$ and $\alpha_2(\omega)$ characterize the scalar, dipole and quadrupole natures, respectively, whose explicit forms have been derived in Ref. 5.

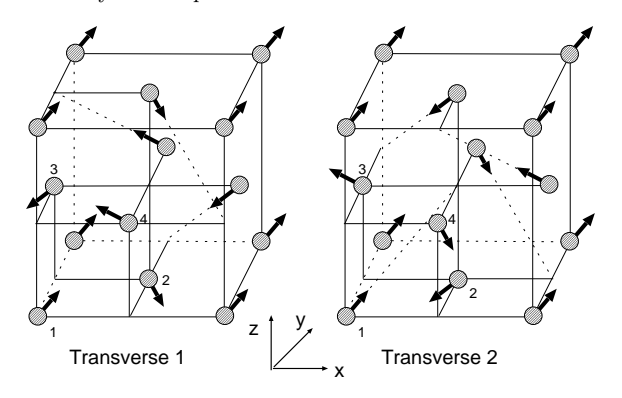


Fig. 1. Two types of the transverse triple-**k** AFM ordering patterns corresponding to a modulation vector $\mathbf{Q} = (001)$. Arrows means vector $(\langle J_x \rangle, \langle J_y \rangle, \langle J_z \rangle)$ and number 1, 2, 3, and 4 specify the sublattices. Oxygen ions are omitted.

3. Application to UO_2 and $U_{0.75}Np_{0.25}O_2$

The ordering pattern at U and Np sites in UO₂ and $U_{0.75}Np_{0.25}O_2$ is believed to be the transverse triple-**k** AFM structure (Fig. 1). The triple-**k** structure is defined by all three members of the star of $\mathbf{k} = \langle 001 \rangle$ simultaneously present on each site. The order parameter vector of the transverse ordering is composed of three transverse waves with different \mathbf{k} 's. There are four sublattices 1, 2, 3 and 4 at (000), $(\frac{1}{2}\frac{1}{2}0)$, $(0\frac{1}{2}\frac{1}{2})$ and $(\frac{1}{2}0\frac{1}{2})$, respectively. Assuming this ordering pattern is materialized, we investigate the energy profile and the azimuthal angle dependence of the RXS spectra at U and Np M_4 edges. Since localized picture provides a good stating point, we construct the ground state of the U ion within the J=4in the f^2 configuration and Np ion within the $J=\frac{9}{2}$ multiplet in the f^3 configuration. Note that due to the strong spin-orbit interaction, these ground multiplets are slightly different from 3H_4 and ${}^4I_{\frac{9}{2}}$ terms, respectively, inferred from the perfect LS coupling.

First, we construct the ground state at U site. Under the influence of the CEF Hamiltonian with cubic symmetry, the ground multiplet J=4 at U site splits into one singlet Γ_1 , one doublet Γ_3 and two triplets Γ_4 and Γ_5 . The lowest levels are made of Γ_5 . Because the values of the CEF parameters and the expansion parameters of the Γ_5 triplet are irrelevant to the following discussion, we relegate the actual expressions of them to the literature.¹⁸ By introducing the dipole operators,

$$J_{p} = \begin{cases} \frac{1}{\sqrt{3}} \left(J_{x} + J_{y} + J_{z} \right) & \text{for} \quad p = 111, \\ \frac{1}{\sqrt{3}} \left(J_{x} - J_{y} - J_{z} \right) & \text{for} \quad p = 1\overline{11}, \\ \frac{1}{\sqrt{3}} \left(-J_{x} + J_{y} - J_{z} \right) & \text{for} \quad p = \overline{1}1\overline{1}, \\ \frac{1}{\sqrt{3}} \left(-J_{x} - J_{y} + J_{z} \right) & \text{for} \quad p = \overline{1}1\overline{1}, \end{cases}$$
(3.2)

we can construct the triple-**k** AFM ordering state within the Γ_5 triplet by assigning one of the eigenstates of J_p 's to each sublattice. Each J_p takes eigenvalues $\pm j_0 \equiv \pm \frac{5}{2}$ and 0. Two types of the relevant transverse ordering patterns are constructed by assigning either one of the eigenstates with eigenvalues $\pm \frac{5}{2}$ of J_{111} , $J_{1\overline{1}\overline{1}}$, $J_{\overline{1}\overline{1}}$ and $J_{\overline{1}\overline{1}}$ to sublattices 1, 2, 3 and 4 and to 1, 4, 2 and 3, respectively (Fig. 1). For each sublattice assigned operator J_p , the direction of the vector $(\langle J_x \rangle, \langle J_y \rangle, \langle J_z \rangle)$, in which the ex-

pectation values are evaluated by the eigenstate of J_p , coincides with that of p.

Note that each dipole operator J_p commutes with the corresponding quadrupole operator Q_p , which is defined by replacing J_x , J_y and J_z in J_p with Q_{yz} , Q_{zx} and Q_{xy} , respectively. Each Q_p could be represented as

$$Q_p = \frac{13}{4} \begin{pmatrix} 1 & 0 & 0 \\ 0 & 1 & 0 \\ 0 & 0 & -2 \end{pmatrix}, \tag{3.3}$$

where the basis are taken by the eigenstates of J_p . It is obvious that the eigenstate of J_p induces the quadrupole moment simultaneously. The eigenstates of J_p 's with eigenvalues $\pm j_0$ and 0 are those of Q_p 's with eigenvalues $\frac{13}{4}$ and $-\frac{13}{2}$, respectively.

ues $\frac{13}{4}$ and $-\frac{13}{2}$, respectively. Similarly, the ground multiplet $J=\frac{9}{2}$ at Np site splits into one doublet Γ_6 and two quartets $\Gamma_8^{(1)}$ and $\Gamma_8^{(2)}$ due to the CEF Hamiltonian. The lowest levels are made of $\Gamma_8^{(2)}$. Each J_p within this subspace takes eigenvalues $\pm j_1$ and $\pm j_2(|j_1| > |j_2|)$. Since the commutation relation $[J_p, Q_p] = 0$ also holds, the eigenstate of J_p induces the quadrupole moment simultaneously. The eigenstates of J_p 's with eigenvalues $\pm j_1$ and $\pm j_2$ are those of Q_p 's with eigenvalues $-q_1$ and $+q_1$, respectively. Details for the AFM ordering at Np site are found in Ref. 5.

Assuming the eigenstates of J_p 's with eigenvalue $-j_0$ (or $+j_0$) at U site and those with $-j_1$ (or $+j_1$) at Np site are realized at each sublattice, we calculate the RXS spectra with $\mathbf{G}=(112)$. Due to the fact that $[J_p,Q_p]=0$, the initial state takes non-zero expectation values of dipole and quadrupole moment. This immediately leads to a possibility that both two energy profiles $\alpha_1(\omega)$ and $\alpha_2(\omega)$ emerge. This is one of the prominent differences when we have investigated the RXS spectra from the triple- \mathbf{k} AFO state in pure NpO₂ where only $\alpha_2(\omega)$ is allowed. For the scattering vector $\mathbf{G}=(hh\ell)$ with $h+\ell=odd$, the interference between $\alpha_1(\omega)$ and $\alpha_2(\omega)$ is expected in the σ - π' (rotated) channel while only the contribution from $\alpha_2(\omega)$ is detected owing to the geometrical factor in the σ - σ' (non-rotated) channel.

In order to evaluate the energy profiles $\alpha_1(\omega)$ and $\alpha_2(\omega)$, we take the intra-atomic Coulomb interaction and the spin-orbit interaction into full account in the preparation of the intermediate state. Details are described in Ref. 5. The value of Γ , the life-time broadening width of the core hole, is taken as 2 eV (HWHM). We display the numerical results in Fig. 2. We adjusted the core hole energy such that the peak is located at the experimental position in the σ - σ' channel. The spectra agree semi-quantitatively well with the experiments. Since we find $|\alpha_1(\omega)|^2$ is much larger than $|\alpha_2(\omega)|^2$, for instance, $|\alpha_1(\omega)|^2 \sim 125|\alpha_2(\omega)|^2$ at the U site and $\sim 192|\alpha_2(\omega)|^2$ at the Np site when $\Gamma = 2$ eV, the interference effect expected in the σ - π' channel is negligible. In experimental data, the peak position in the σ - π' channel is higher than that in the σ - σ' channel about 2.0 eV at U site and 0.3 eV at Np site. Our results, 1.3 eV and 0.27 eV, respectively, capture such tendency. The difference between the spectral shape at U site and that at Np site is not prominent due to the large value of $\Gamma = 2$ eV. When

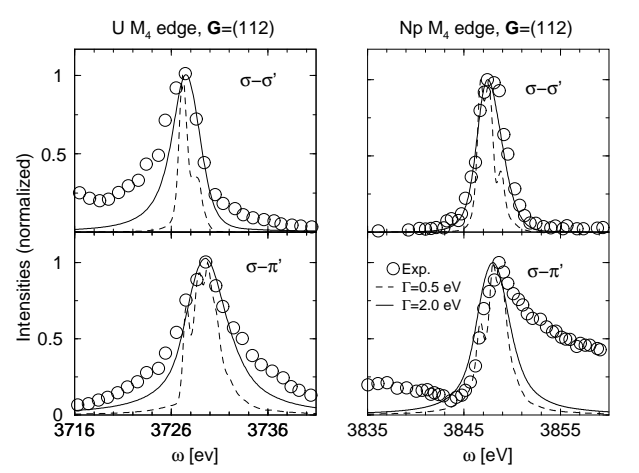


Fig. 2. The RXS spectra as a function of the photon energy at $\mathbf{G} = (112)$ around U and Np M_4 edges. Solid and broken lines are calculated from the transverse triple- \mathbf{k} AFM phases at U (left) and Np (right) sites with $\Gamma = 2.0$ and 0.5 eV, respectively. The upper and lower panels are the spectra in the σ - σ' and σ - π' channels, respectively. The experimental data are taken from Wilkins et al. (open circles). All the peak heights are normalized.

 Γ is reduced around 0.5 eV, the spectra show multi-peak structure which could distinguish those at U from Np sites when the drastic improvement of the absorption correction technique would been achieved.

Fig. 3 shows the azimuthal angle dependence of the peak intensity expected from the transverse triple-k AFM phase with G = (112). The spectra are evaluated by incoherent addition of the contributions from two transverse ordering patterns. Since $\alpha_1(\omega)$ contribution dominates the whole intensity in the σ - π' channel, we plot the ψ dependence of the pure $\alpha_1(\omega)$ in this channel (Fig. 3 (b)). Experimental data in Fig. 3 (a) are those of U in UO_2 and those of Np in $U_{0.75}Np_{0.25}O_2$. ^{10,11} The overall agreement between the experimental data and the theoretical curve is interpreted as one of the evidences of the realization of the triple-k structure in these materials as the experimentalists have suggested. 10,11 Notice that no ψ dependence has been detected in the σ - π' channel around U and Np M_4 edges in $U_{0.75}Np_{0.25}O_2$. ^{10,19} Our calculation, however, reveals that this channel should possess the ψ dependence although the dependence is mild around $\psi = -\pi/2 \sim 3\pi/4$ as shown in Fig. 3 (b). The detailed experimental information, in particular, around $\psi = \pi$ will clarify this discrepancy. Note that, in the E1 transition, quadrupole profile $\alpha^{(2)}(\omega)$ alone has contribution, if any, on the spectrum in the $sigma-\sigma'$ channel. We have confirmed that the ψ dependence (not shown) in this channel expected from the longitudinal triple-k AFQ phase is completely different from that of the observed one. Therefore, it excludes a possibility of any types of the longitudinal triple-k orderings, such as the AFM, AFQ and AFO phases.

4. Summary

We have utilized the useful expression of the RXS amplitude derived in Ref. 5 to investigate the RXS spectra at U and Np M_4 edges in UO₂ and U_{0.75}Np_{0.25}O₂, as-

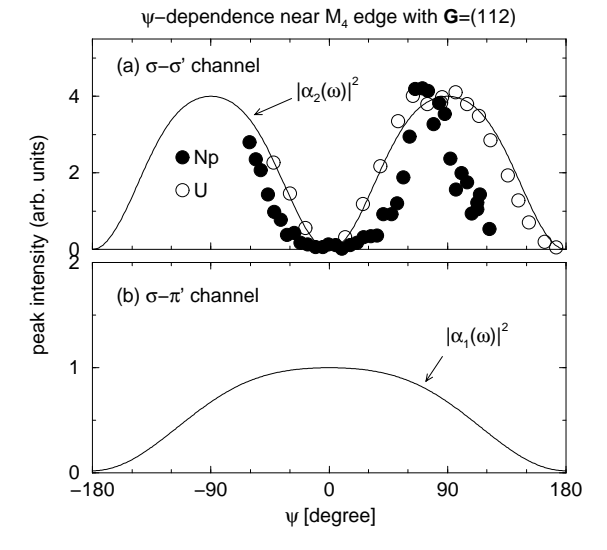


Fig. 3. Azimuthal angle (ψ) dependence of the peak intensity near U and Np M_4 edges at $\mathbf{G} = (112)$ in the transverse triple- \mathbf{k} AFM phase. (a) ψ dependence of $|\alpha_2(\omega)|^2$ in the σ - σ' channel. Open and filled circles are experimental data near U M_4 edge in UO₂ (Ref. 11) and Np M_4 edge in U_{0.75}Np_{0.25}O₂ (Ref. 10), respectively. (b) ψ dependence of $|\alpha_1(\omega)|^2$ in the σ - π' channel.

suming the transverse triple-**k** AFM ordering phase is substantiated in these materials. Our analysis has shown the semi-quantitative agreement with the experimental data, meaning that the spectra in the σ - σ' and σ - π' channels characterize the quadrupole ($|\alpha_2(\omega)|^2$) and dipole ($|\alpha_1(\omega)|^2$) natures, respectively, as the experimentalists had suggested. A discrepancy of the azimuthal angle dependence in the σ - π' channel between the experiments and our theory should be addressed on the future study.

This work was partially supported by a Grant-in-Aid for Scientific Research from the Ministry of Education, Science, Sports and Culture, Japan.

- 1) E. D. Isaacs et al.: Phys. Rev. Lett. 65 (1990) 3185.
- D. Mannix et al.: Phys. Rev. B 60 (1999) 15187.
- 3) J. A. Paixão et al.: Phys. Rev. Lett. 89 (2002) 187202.
- 4) N. Bernhoeft et al.: Acta Physica Pol. B 34 (2003) 1367.
- 5) T. Nagao and J. Igarashi: Phys. Rev. B **72** (2005) 174421.
- J. P. Hannon, G. T. Trammell, M. Blume, and D. Gibbs: Phys. Rev. Lett. 61 (1988) 1245: *ibid.* 62 (1989) 2644(E).
- J. Luo, G. T. Trammell, and J. P. Hannon: Phys. Rev. Lett. 71 (1993) 287.
- 8) S. W. Lovesey and E. Balcar: J. Phys.:Condens Matter 8 (1996)
- 9) T. Nagao and J. Igarashi: J. Phys. Soc. Jpn., 74 (2005) 765.
- 10) S. B. Wilkins et al.: Phys. Rev. B 70 (2004) 214402.
- 11) S. B. Wilkins et al.: Phys. Rev. B **73** (2006) 060406.
- P. Burlet, J. Rossat-Mignod, S. Quezel, O. Vogt, J. C. Spirlet and J. Rebizant, J. Less-Common Met., 121 (1986) 121.
- 13) R. Caciuffo et al.: Phys. Rev. B 59 (1999) 13892.
- 14) R. Caciuffo et al.: J. Phys.: Condens. Matter 15 (2003) S2287.
- 15) Y. Tokunaga et al.: Phys. Rev. Lett. **94** (2005) 137209.
- 16) K. Kubo and T. Hotta: Phys. Rev. B 71 (2005) 140404(R).
- 17) A. Kiss and P. Fazekas: Phys. Rev. B 68 (2003) 174425.
- 18) G. Amoretti et al.: Phys. Rev. B 40 (1989) 1856.
- 19) As for U site in UO₂ in Ref. 11, unfortunately, we cannot find any description about the ψ dependence in the σ - π' channel.